Bull Math Biol
DOI 10.1007/s11538-011-9663-3

ORIGINAL ARTICLE

A Mathematical Model for the Effects of HER2 Over-Expression on Cell Cycle Progression in Breast Cancer

Amina Eladdadi · David Isaacson

Received: 1 May 2009 / Accepted: 28 April 2011

Abstract In this paper, we present a mathematical model predicting the fraction of proliferating cells in G1, S, and G2/M phases of the cell cycle as a function of EGFR and HER2. We show that it is possible to find parameters for the mathematical model so that its predictions agree with the experimental observations that HER2 over-expression results in: (1) a shorter G1-phase and early S-phase entry; (2) and that with a 1-to-1 ration between EGFR and HER2, the growth advantage in HER2 over-expressing cells is indeed associated with the increase of the HER2 expression level.

Keywords HER2 · EGFR · Cell cycle · Cell proliferation · Receptor modeling · Mathematical modeling · Breast cancer · HER2 over-expression

1 Introduction

Over-expression of the Human Epidermal growth factor Receptor 2, HER-2 (also known as neu/ErbB2), generally due to the amplification of the HER2/neu gene, is observed in approximately 30% of human breast cancers. Also, HER-2 over-expression correlates with a shorter survival rate and short time to relapse in breast cancer patients (Slamon et al. 1987). HER2 is a transmembrane tyrosine kinase receptor which belongs to the HER family of four epidermal growth factor receptors (EGFR/ErbB1, HER-2/ErbB2, HER-3/ErbB3, HER-4/ErbB4), and is involved

A. Eladdadi (✉)
The College of Saint Rose, 432 Western Avenue, Albany, NY 12203, USA
e-mail: eladdada@strose.edu

D. Isaacson
Department of Mathematical Sciences, Rensselaer Polytechnic Institute, Troy, NY 12180, USA
e-mail: isaacd@rpi.edu

Published online: 05 August 2011

in signal transduction pathways that regulate cell growth, proliferation, cell survival, angiogenesis, and cell motility (reviewed in Hynes et al. 2001; Yarden and Sliwkowski 2001). HER receptors are activated by a large group of ligands that can be divided into two groups (EGF-like ligands and neu differentiation factors) based on their binding specificities (Riese and Stern 1998; Salomon et al. 1995; Yarden and Sliwkowski 2001). Unlike the other HER family members, HER2 does not directly bind any ligand with high affinity. Instead, it relies on lateral-interaction with other HER family members for its complete activation (Klapper et al. 1999). Although all of the HER family receptors are capable of dimerizing with each other, HER2 is the preferred dimerization partner in cancer. HER2-containing dimers have increased signaling potency relative to dimers that do not contain HER2. This is mainly because HER2 is able to decrease the rate of ligand dissociation from its dimerized partner, HER2-containing heterodimers have a slower rate of endocytosis and a higher rate of recycling back to the cell surface. These features translate to potent mitogenic and antiapoptotic signals (Brennan et al. 2000; Graus-Porta et al. 1997; Hynes 2005; Worthylake et al. 1999; Yarden and Sliwkowski 2001).

One of the major cellular processes affected by HER2 signaling is the cell cycle. The molecular mechanism underlying how oncogenic signals of HER-2/neu affect the cell cycle machinery is not completely determined. The biological consequence of HER2 over-expression is a shortening of the G1-phase of the cell cycle and early S-phase entry, which leads to hyper-proliferation (Hynes et al. 2001; Timms et al. 2002). Numerous experimental studies show that increased HER2 signaling, resulting from the receptor over-expression, contributes to the deregulation of the G1/S transition (Hynes 2005; Hynes et al. 2001; Le et al. 2005; Timms et al. 2002). Progression through G1-phase and entry into S-phase is regulated by the activation of G1-phase cyclin-dependent kinases (CDKs). HER2 over-expression has been correlated with the up-regulation of these CDKs, particularly cdk6 and cyclins D1 and E, and enhanced degradation and relocalization of p27Kip1 one of the G1-phase cyclin-dependent inhibitors. An increase in p27Kip1 protein causes proliferating cells to exit from the cell cycle, whereas a decrease in p27Kip1 protein promotes quiescent cells to resume cell proliferation (see Hynes 2005; Hynes et al. 2001; Le et al. 2003; Neve et al. 2000 and references therein).

The oncogenic nature of HER2 over-expression and the accessible location of the HER2 on the cell surface, where it can interact with ligands and antibodies, makes it an ideal target for tumor-specific therapy. A number of strategies have been evaluated for inhibiting the growth of cells that over-express HER2, including the use of the humanized anti-HER2 monoclonal antibody trastuzumab (Herceptin) directed against the extracellular domain of the HER2 (Hynes 2005; Yarden and Sliwkowski 2001). The mechanisms by which trastuzumab induces regression of HER2-over-expressing tumors are still being investigated. Several molecular and cellular effects of trastuzumab on the HER2 over-expressing cells have been reported in the literature including its effects on the cell cycle (Cai et al. 2008). Several experimental studies showed that cells treated with trastuzumab undergo arrest during the G1 phase of the cell cycle by increasing p27Kip1 protein, which halts cell proliferation (Lane et al. 2001; Le et al. 2003, 2005; Neve et al. 2000; Timms et al. 2002). Many chemotherapeutic agents are cell cycle specific, and they

have their greatest effect on cells in certain phases of the cell cycle (see, for example, Cojocaru and Agur 1992; Gorelik et al. 2008 and references therein). Therefore, characterizing the progress of the cell cycle of cancer cell is of great importance in cancer management.

To investigate the effects of HER2 over-expression on cell cycle progression, we have developed a mathematical model that describes the cell cycle transition rates of HER2-over-expressing cells as a function of the HER2 and EGFR expression level. Building on our earlier mathematical model (Eladdadi and Isaacson 2008), the cell cycle model is an extension of the cell proliferation model which treated HER2-positive cancer cells as a lumped mass, and no distinction was made between cancer cells. In order to characterize these effects, we use a three-compartment cell cycle model with nonconstant transition rates. Our new hypothesis is that the transition rates depend on the number of the cell surface HER2 and EGFR receptors and their signaling properties. The model enables us to simulate the transition rates of the HER2 over-expressing cells as they progress through their cell cycle with various HER2 and EGFR expression levels at various EGF ligand concentrations. Of particular interest, is the G1/S transition rate since it has been established experimentally that HER2 over-expression results in a shorter G1-phase and an early S-phase entry (Harris et al. 1999; Hynes et al. 2001; Le et al. 2005; Timms et al. 2002). The model also allows the prediction of the cell population growth as a function of HER2 and EGFR receptors numbers.

This paper is organized as follows: Sect. 2 presents a background on the cell cycle and cell cycle models. The mathematical model is introduced in Sect. 3. Parameters estimates and model validation is discussed in Sect. 4. In Sect. 5, simulation results and model predictions are presented. The paper concludes with a discussion in Sect. 6, summarizing our main results, and suggesting possible directions for future work.

2 Background

2.1 Cell Cycle Phases

Cell cycle dynamics are closely connected to cell growth and to the mechanism of controlling cell proliferation. The cell cycle was first described by Howard and Pelc in the early 1950s (Howard and Pelc 1951), and can be defined as an ordered set of biochemical events resulting in cell division. The sequence of these events is divided into four phases: the G1 phase (growth also known as first gap), followed by the S phase (synthesis), G2 phase (second growth), and the M phase (mitotic). In the G1-phase, ribonucleic acid (RNA) and proteins are synthesized in preparation of DNA synthesis. In the S-phase, the cell undergoes DNA synthesis. At the end of the S-phase, DNA synthesis is complete and the cell has doubled its genetic material. Cells replicate their DNA, creating two identical copies so that each daughter cell can each inherit an exact copy. In G2-phase, the cell continues to grow and synthesize all the proteins that the daughter cells need after division. Finally, in the M-phase, the cell separates its DNA and divides into two. On completion of M-phase, two daughter

cells are produced with the equivalent genetic capacity of the previous parent cell. Each daughter cell may reenter G1 to begin the cycle again, or enter a resting state (quiescent), called G0. A cell may remain in this state for many years, but can reenter the cycle at the first gap (G1) phase when stimulated, i.e., following binding of a growth factor to its extracellular receptor. A more detailed description of the cell cycle can be found in Alberts et al. (2002).

2.2 Cell Cycle Models

Cell cycle models have been proposed to characterize the proliferative nature of cancer, and to model the effects of the drugs used in chemotherapy in a more comprehensive way (reviewed in Araujo and Mcelwain 2004). These models explicitly represent the transition of cells between the different phases of the cell cycle. Most cell cycle models use multicompartmental analysis. The compartment is analogous to the phase of the cell cycle (i.e., G0/G1/S/G2/M) and as the cell progresses through the cell cycle, it spends time in each compartment.

The phases of the cell cycle could be grouped depending on the details in the mathematical model. The simplest and more detailed multi-compartment models divide the cell cycle into two or three compartments. Multicompartment models explicitly represent the transition of cells between each phase of the cell cycle.

The main considerations in cell cycle modeling are the estimation of the model parameters and the characterization of the parameters that should be altered to mimic the (perturbed/unperturbed) cell line kinetics. Known clinical information about the growth kinetics of cancer cells can usually be obtained from the experimental literature such as flow cytometry studies. This information includes: cell-cycle time, doubling time, proliferative fraction, time in resting phase, and the percentage of cells in each phase of the cell cycle.

2.2.1 Population Doubling Time

Experimental estimates of the cell population doubling time T_d in vitro can be made from direct time series measurement of the cell number (e.g., by Coulter counters) of the population under study. In vitro, when cell loss is negligible, proliferation rates are more directly deduced from the doubling time by simple fittings to the experimental data. In vivo, in solid tumors, T_d estimates rely on the evaluation of tumor diameters using calipers (transformed into 'tumor mass' with simple formula) or on imaging techniques such as X-ray tomography and magnetic resonance (Basse et al. 2005). In this study, the doubling time of the parental cell line (HB4a) was taken from experimental data (Harris et al. 1999; Timms et al. 2002) and the doubling time for its HER2 over-expressing clone (C3.6) was taken from numerical estimates in our previous study (Eladdadi and Isaacson 2008).

2.2.2 Cell Cycle Fraction

While understanding cellular proliferation at this level is important, acquiring data characterizing the fraction of cells in the different phases is nontrivial. In order to

determine the fraction (or the percentage) of cells at different phases of the cell cycle, samples must be obtained and stained for DNA and RNA content at different points in time. Based on the amount of DNA or RNA in different cells, the fraction of cells in a specific phase can be determined (Shapiro 2003). In the case of this study, the flow cytometry data from Timms' paper (Timms et al. 2002) and computer simulation are used to compute the cell cycle fractions %G1, %S, and %G2M (percentage of cells in G1-, S-, G2M-phases, respectively). The transition rate constant λ_3, from S-phase to G2M-phase is computed using the experimentally measured quantities (flow cytometry data). Whereas the G1/S transition rate, λ_1, and the S/G2 transition rate, λ_2, are estimated from various simulations.

2.2.3 Cell Cycle Time

The average time required for a cell to perform an entire cell cycle successively is defined as the cell cycle time, denoted by T_c. The cell cycle duration is also defined as the sum of the average time spent in each phase: $T_c = T_{G1} + T_S + T_{G2} + T_M$. Here T_{G1}, T_S, T_{G2}, and T_M are the average times spent in G1, S, G2, and M phases, respectively. The transition from G2-phase to M-phase is short and cannot easily be measured (by flow cytometry), for this the average time spent in phase G2 and phase M is combined into one time, T_{G2M}. Thus, the cell cycle can be rewritten as: $T_c = T_{G1} + T_S + T_{G2M}$. The relationship between the kinetic parameters (T_{G1}, T_S, and T_{G2M}, and their sum T_c) and the percentages of cells in the various phases was first established by Steel (1977), also called Steel's formula and is given as follows:

$$T_c = T_d, \tag{1a}$$

$$T_{G2M} = T_c \frac{\ln(\frac{\%G2M}{100} + 1)}{\ln 2}, \tag{1b}$$

$$T_S = T_c \frac{\ln(\frac{\%S+\%G2M}{100} + 1)}{\ln 2} - T_{G2M}, \tag{1c}$$

$$T_{G1} = T_c - T_{G2M} - T_S \tag{1d}$$

where T_d is the doubling time of the cell population, and %G1, %S, and %G2M are the percentage of cells in G1-phase, S-phase, and G2M-phase, respectively. Steel's equations (1) are valid if there is no variability, i.e., if every cell is considered to spend exactly a time T_{G1} in G1, a time T_S in S-phase, and a time T_{G2M} in the phase G2M. The transition rate between cell cycle phases (λ_i's) is defined as follows (Takahashi 1968):

$$\lambda_{G1} = \frac{1}{T_{G1}}, \qquad \lambda_S = \frac{1}{T_S}, \qquad \lambda_{G2M} = \frac{1}{T_{G2M}}. \tag{2}$$

3 Model Development

In this section, we formulate a mathematical model to study the effects of HER2 over-expression on the cell cycle progression. The model formulation is based on

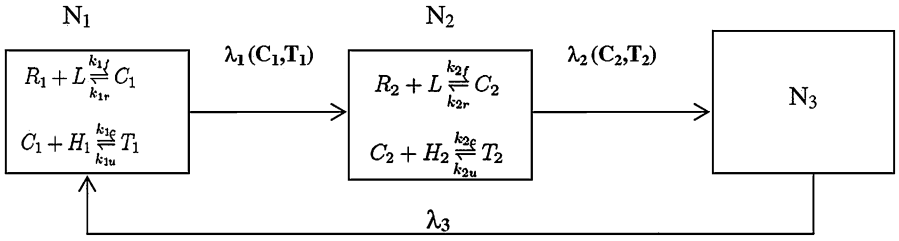

Fig. 1 The three compartment cell cycle model (where R_i, H_i represent the EGFR and HER2 in compartment i respectively)

the effects of HER2 over-expression on the cell cycle as described experimentally in Timms et al. (2002). The different components of the model are discussed below along with the underlying assumptions. In Sect. 3.1, the interactions of the EGFR and HER2 in G1- and S-phases are presented. We derive the cell population dynamics in each cell cycle phase in Sect. 3.2. The new feature of the model is the dependence of the transition rates on the kinetics properties of the EGFR and HER2; this is specified in Sect. 3.3. The model is summarized in Sect. 3.4. The definitions of all the model variables and parameters are summarized in Table 1 and Table 3, respectively. This cell cycle model expands on our previous cell proliferation model. For detailed derivation of the model's equations, the reader is referred to Eladdadi and Isaacson (2008).

3.1 Receptor–Ligand Interactions

We divide the HER2-positive cell population into three compartments. G1-phase ($N_1(t)$), S-phase ($N_2(t)$), and G2/M-phase ($N_3(t)$), where $i = 1, 2, 3$ correspond to compartments 1, 2, and 3, respectively as depicted in Fig. 1. We based our grouping on the available experimental data investigating the effects of HER2 over-expression on the cell cycle. These data show that HER2 over-expression affect the cell transition from G1-phase to S-phase (Harris et al. 1999; Hynes et al. 2001; Le et al. 2005; Neve et al. 2000; Timms et al. 2002; Yarden and Sliwkowski 2001). We consider the cell surface EGFR and HER2 in each phase of the cell cycle. We assume that the cell surface EGFR and HER2 in compartment 3 are negligible, this is likely due to their entire internalization at the G2M phase.

The cells in G1- and S-phases are represented by the first and second compartment of the model, respectively. In these compartments, the binding of EGFR and HER2 is described by the following system of ODEs:

$$\frac{dC_i}{dt} = k_{if}(r_i N_i - C_i - T_i)L - k_{ir}C_i - k_{ic}(h_i N_i - T_i)C_i + k_{iu}T_i, \tag{3a}$$

$$\frac{dT_i}{dt} = k_{ic}(h_i N_i - T_i)C_i - k_{iu}T_i. \tag{3b}$$

Here, T_i is the number of ternary complexes and C_i is the total number of binary (EGFR-EGF)receptors, in compartment i. The rate of change in ligand concentration

is defined as the total rate of change in ligand concentration in both compartments 1 and 2. We did not account for ligands in compartment 3 (G2M-phase) since the receptor activities are supposedly negligible in G2M-phase. The following equation describes the rate of change of the total ligand concentration:

$$\frac{dL}{dt} = \left(-k_{1f}(r_1N_1 - C_1 - T_1)L + k_{1r}C_1\right) + \left(-k_{2f}(r_2N_2 - C_2 - T_2)L + k_{2r}C_2\right) + S_L - \lambda_d L. \tag{4}$$

Here, $L(t)$ denotes the concentration in moles per liter of the EGF ligand.

3.2 Cell Population Dynamics

The transit times of cells through phases of the cell cycle vary particularly in cancer cells. In the simplest models, an exponential distribution is used to model the transit times. The expected number of cells exiting the ith compartment is given by $-\lambda_i N_i(t)$, where λ_i is a positive constant representing the transition rate (1/time) from the ith compartment. Cells can be lost (apoptosis) from either compartment with a particular death rate. If we assume that no external stimuli are present and we neglect the natural death, the inflow of one compartment equals the outflow of the other, and thus the rate of change of the cell population can be represented mathematically by performing mass balances over each compartment. If the transition rates λ_i are constant, the system describing the compartmental cell population dynamics is linear and can be described using the system of (5) with constant transition rates:

$$\frac{dN_1(t)}{dt} = -\lambda_1 N_1(t) + 2\lambda_3 N_3(t), \tag{5a}$$

$$\frac{dN_2(t)}{dt} = \lambda_1 N_1(t) - \lambda_2 N_2(t), \tag{5b}$$

$$\frac{dN_3(t)}{dt} = \lambda_2 N_2(t) - \lambda_3 N_3(t). \tag{5c}$$

The factor 2 in (5a) represents the cell division which describes the flow from the third into the first compartment.

The question we are investigating in this study is how HER2 over-expression affect the cell proliferation rate as the cell progresses through its cell-cycle phases. Another aspect of studying the cell cycle is the treatment of cancers with chemotherapeutic agents. We want to know for instance, if a monoclonal antibody targeting HER2 is to be administered, in which phase of the cell cycle it will be more beneficial. Also, we would like to know in which order anticancer drugs are to be given, which in turns depends on the position of the cell in the cell-cycle. The simple three cell cycle model with constant transition rates is not able to answer these questions. Therefore, we propose that the transition rates λ_1 and λ_2, be a function of the HER2 and EGFR numbers and their kinetics properties. Due to the lack of experimental data, we assume that the expression levels of HER2 is different in G1-phase and

S-phase. Similarly, we assume that the expression levels of EGFR receptors is different in both compartments. By including the dynamics of the cell surface receptors in the model, the cell cycle model is well poised to predict the experimental results by Hynes (2005), Timms et al. (2002) as well as to answer some of these questions.

3.3 Transition Rates

A novel feature of this model is the incorporation of the EGFR and HER2 binding kinetic properties into the transition rates. We define the transition rates λ_i, where $i = 1, 2$ denote the cell cycle compartments G1-phase and S-phase respectively, as a weighted sum of the signaling forms of the HER2 and EGFR receptors and their cell surface binary (C_i) and ternary (T_i) complexes. λ_i is then defined as follows:

$$\lambda_i(C_i, T_i) = A_i f(C_i) + B_i f(T_i). \tag{6}$$

As a first approximation, we choose f to be a monotonic saturating function: $f(a, b, x) = \frac{ax}{b+x}$. Thus the functional λ_i is expressed as

$$\lambda_i(C_i, T_i) = A_i f\left(\alpha_i^1, \beta_i^1, C_i(t)\right) + B_i f\left(\alpha_i^2, \beta_i^2, T_i(t)\right). \tag{7}$$

Here:

- A_i and B_i are balancing factor in phase i (the contribution of each receptor to the signaling networks)
- α_i^1 and α_i^2 (1/time) are the maximum transition rates in phase i
- β_i^1 and β_i^2 (#/volume) are the number of cell surface complexes in phase i required to generate a half-maximal response.

3.4 The Cell Cycle Model Summary

Combining the system of equations of receptor-ligand binding: (3a), (3b), and (4), the cell cycle population dynamics (5), along with the new definition of the transition rates (7), we get the cell cycle model for the whole cell population. The model describes the relationship between the cell surface receptors HER2 and EGFR in each compartment and the transition rates as the cell progresses through its cell cycle and is given by the following system:

$$\frac{dC_1}{dt} = k_{1f}(r_1N_1 - C_1 - T_1)L - k_{1r}C_1 - k_{1c}(h_1N_1 - T_1)C_1 + k_{1u}T_1, \tag{8a}$$

$$\frac{dT_1}{dt} = k_{1c}(h_1N_1 - T_1)C_1 - k_{1u}T_1, \tag{8b}$$

$$\frac{dC_2}{dt} = k_{2f}(r_2N_2 - C_2 - T_2)L - k_{2r}C_2 - k_{2c}(h_2N_2 - T_2)C_2 + k_{2u}T_2, \tag{8c}$$

$$\frac{dT_2}{dt} = k_{2c}(h_2N_2 - T_2)C_2 - k_{2u}T_2, \tag{8d}$$

Table 1 A summary of variables used in the model (8a)–(8h)

Variable	Description	Initial value	Units	Source
C_i	Number of the binary receptor ligand (EGFR-EGF) complexes in phase i	0	#/volume	–
T_i	Number of the ternary (EGFR-EGF-HER2) complexes in phase i	0	#volume	–
L	Ligand concentration	1	μM	Harris et al. (1999), Timms et al. (2002)
N_1	Cell density in G1-phase	0.5×10^6	#/volume	Harris et al. (1999), Timms et al. (2002)
$N_i, i = 2, 3$	Cell density in S- and G2M-phase, respectively	0	#/volume	Harris et al. (1999), Timms et al. (2002)
$h_i, i = 1, 2$	The total cell surface HER2 receptors	varies	#/cell	Harris et al. (1999), Timms et al. (2002)
$r_i, i = 1, 2$	The total cell surface EGFR receptors	varies	#/cell	Harris et al. (1999), Timms et al. (2002)

$$\frac{dL}{dt} = -k_{1f}(r_1N_1 - C_1 - T_1)L + k_{1r}C_1 - k_{2f}(r_2N_2 - C_2 - T_2)L + k_{2r}C_2 + S_L - \lambda_d L, \tag{8e}$$

$$\frac{dN_1}{dt} = -\left(A_1\frac{\alpha_1^1 C_1}{\beta_1^1 + C_1} + B_1\frac{\alpha_1^2 T_1}{\beta_1^2 + T_1}\right)N_1 + 2\lambda_3 N_3, \tag{8f}$$

$$\frac{dN_2}{dt} = \left(A_1\frac{\alpha_1^1 C_1}{\beta_1^1 + C_1} + B_1\frac{\alpha_1^2 T_1}{\beta_1^2 + T_1}\right)N_1 - \left(A_2\frac{\alpha_2^1 C_2}{\beta_2^1 + C_2} + B_2\frac{\alpha_2^2 T_2}{\beta_2^2 + T_2}\right)N_2, \tag{8g}$$

$$\frac{dN_3}{dt} = \left(A_2\frac{\alpha_2^1 C_2}{\beta_2^1 + C_2} + B_2\frac{\alpha_2^2 T_2}{{\beta_2}^2 + T_2}\right)N_2 - \lambda_3 N_3. \tag{8h}$$

In the absence of the ligand, the variables $C_i(t)$ and $T_i(t)$ $(i = 1, 2)$ are zero since the formation of complexes require the ligand to be present. Furthermore, because we are only considering the ligand-dependent cell growth, N_i $(i = 1, 2, 3)$ is time-invariant in the absence of any initial ligand. So, the initial conditions for the new cell cycle model are

$$C_i(0) = 0, \qquad T_i(0) = 0, \qquad L(0) = L_0, \qquad N_i(0) = N_{i0}, \quad i = 1, 2, 3. \tag{9}$$

To reduce computations, we assume that $\alpha_i^1 = \alpha_i^2$, $\beta_i^1 = \beta_i^2$, and $B_i = 1 - A_i$. The definitions and base values of all the model variables and parameters are summarized in Table 1 and Table 3, respectively.

4 Parameter Estimates and Model Validation

In this section, we estimate the parameter values, which are listed in Table 3. To quantitatively analyze our cell cycle model, we first need to determine the model

Table 2 Flow cytometry data for HB4a and C3.6 cells treated with EGF (Timms et al. 2002)

Time (hours)	HB4a			C3.6		
	%G1	%S	%G2M	%G1	%S	%G2M
24	66	15	18	45	23	32
36	66	11	23	45	15	40
48	71	10	19	48	20	32
Exponential growth	57	11	32	37	16	47

parameter values or at least a reasonable physiological range for them. We use data from the available literature where possible and for other parameters we consider different value ranges and their impact on the model outputs. The experimental data used to validate our model is presented in Sect. 4.1, followed by a description on parameter estimates in Sect. 4.2.

4.1 Experimental Data

To validate our three compartment cell cycle model, we used cell cycle flow cytometry data (Fig. 1C) in Timms et al. (2002). This study was designed to investigate the effects of HER2 over-expression on the cell cycle of the luminal epithelial cell line HB4a and its HER2-over expressing clone C3.6. Timms et al. (2002) analyzed the DNA content of HB4a and C3.6 cells, comparing exponentially growing (10% FCS), serum-starved, and mitogen-treated (HRGb1, EGF, or 10% FCS) cells. Their data show that HER2 promotes mitogen-stimulated S phase entry, and that HER2 over-expression in breast luminal epithelial cells results in early S phase entry following mitogen treatment. The experimental results by Timms and coworkers were consistent with earlier studies by Hynes et al. (2001), Neve et al. (2000), Yarden and Sliwkowski (2001), which show that HER2 over-expression results in a shortening of the G1 phase of the cell cycle and early S phase entry, which in turns, leads to hyper-proliferation. The flow cytometry data from Timms' paper is extracted and summarized in Table 2.

4.2 Parameter Value Selection

Parameters that match experimental data were found by trial and error. We used the doubling time as an indicator of a good fit for the data. The doubling time for the parental cell lines HB4a is approximately 48 hours as in experiments (Harris et al. 1999; Timms et al. 2002), and for its HER2 expressing cell line C3.6 is approximately 42 hours as shown numerically in Eladdadi and Isaacson (2008). The kinetic rate constants (k_f, k_r, k_c, k_u) for receptor-ligand binding have been adapted from the parameter set proposed by Hendriks et al. (2003a, 2003b), which is based on the most up-to-date experimental data available for the EGFR/HER2 receptor-ligand binding. Estimates for some of the parameter values have been determined on the basis of the available experimental details (e.g., cell cycle phase times, T_{G1}, T_S, and T_{G2M}) as discussed below. The remaining parameter values have been fitted to produce results that are feasible in light of available experimental data.

Table 3 A summary of parameters used in the model (8)

Parameter	Definition	Base value	Notes
A_i	Balancing factor in phase i	0–1	Sects. 3.3, 4.2.2
B_i	Balancing factor in phase i	0–1	Sects. 3.3, 4.2.2
S_L	Synthesis rate of ligand in phase i	1×10^7 Mol/min	Hendriks et al. (2003a, 2003b)
k_{if}	Rate constant for association of receptor-ligand complexes in phase i	9.7×10^7 M^{-1} min^{-1}	”
k_{ir}	Rate constant for dissociation of receptor-ligand complexes in phase i	0.24 min^{-1}	”
k_{ic}	Rate constant for ternary complex coupling in phase i	$(10^{-3}\#/cell)^{-1}$ min^{-1}	”
k_{iu}	Rate constant for ternary complex uncoupling in phase i	10 min^{-1}	”
$\alpha_i^{1,2}$	Maximum transition rate in phase i	estimated	Sects. 3.3, 4.2.2
$\beta_i^{1,2}$	Number of cell surface complexes in phase i required to generate a half-maximal response	estimated	Sects. 3.3, 4.2.2
λ_d	Degradation rate of ligand	0.0 Mol/min	Sect. 3.1
λ_i^j	Transition rate of cells from phase i	simulated	Sects. 3.3, 4.2.2

4.2.1 Transition Rate Values

To perform the numerical simulations, we need to get an idea about a valid range for the transition rate constants between G1-phase and S-phase (λ_1), S-phase and G2M-phase (λ_2), and G2M-phase and G1-phase (λ_3) for both the parental cells HB4a and its clone cells C3.6. The values of these transition rate constants are not available in the literature. To this end, we used Steel's equations (1) which give the relationship between the cell cycle phase times and the percentages of cells in each phase of the cell cycle. This is a valid approximation since HB4a and C3.6 cells exhibit asynchronous exponential growth also known steady DNA distributions (see Basse et al. 2005 and Harris et al. 1999 and references therein). Using the experimental values of %G1, %S, and %G2M (Table 2), we are able to compute the cell cycle phase times (in hour) for the parental cells HBA4a ($T_{G1} = 23.23$, $T_S = 5.54$, $T_{G2M} = 19.22$), and its clone C3.6 ($T_{G1} = 12.40$, $T_S = 6.26$, $T_{G2M} = 23.34$). Then, substituting these cell cycle time values into (2), we obtain the following transition rate values for HB4a cells: ($\lambda_1 = 0.0430$, $\lambda_2 = 0.1804$, $\lambda_3 = 0.0520$) and for its clone C3.6 cells: ($\lambda_1 = 0.0807$, $\lambda_2 = 0.1597$, $\lambda_3 = 0.0428$). The units of the transition rate constants are per hour.

4.2.2 Other Parameter Values

Here, we summarize the other parameter values estimates:

- The maximum transition rate constants α_i^1 and α_i^2 (where $i = 1, 2$ denotes G1-phase or S-phase, and the superscripts 1 and 2 are for HB4a and C3.6, respectively), have been estimated from information provided in our previous paper (Eladdadi and Isaacson 2008). We varied these rate constants over a wide range of values as described in the simulation results section. Parameters α_i^1 and α_i^2 are model input and are the same for the parental cell line HB4a and its HER2 over-expressing clone C3.6 since they are a characteristic of the intrinsic cell growth signaling network and do not depend on the expression levels of the receptors. We assume that $\alpha_i^1 = \alpha_i^2$ to reduce computations.
- The number of complexes $(C(t))$ and $(T(t))$ needed to generate half-maximal response, β_i^1 and β_i^2 (where $i = 1, 2$ denotes G1-phase or S-phase, and the superscripts 1 and 2 are for HB4a and C3.6, respectively) are varied over a range of 1,300 and 4,300 receptors/cell as estimated in Eladdadi and Isaacson (2008). These parameters are model input and are the same for the parental cell line HB4a and its HER2 over-expressing clone C3.6. We also assume that $\beta_i^1 = \beta_i^2$ to reduce computations.
- The nonnegative constants, A_i and B_i $(B_i = 1 - A_i)$ (where $i = 1, 2$ denotes G1-phase or S-phase), which give the relative contribution of each signaling receptor to the total proliferation activity are varied between 0 and 1.
- Cell density is expressed as an exponential function of time. The cell population growth experiments are simulated over a period of 48 hours with an initial cell density $N(0) = 0.5 \times 10^6$ cells/liters. The EGF ligand concentration is held constant throughout this simulation to $[EGF] = 1$ μM, the same conditions as in experiments published in Harris et al. (1999), Timms et al. (2002).
- The initial number of EGFR cell-surface receptors is 200,000 per cell; this is representative of the number of EGFR receptors found on human mammary epithelial cells used in experimental studies (Hendriks et al. 2003a, 2003b). The initial number of HER2 cell-surface receptors is varied between 10,000 (normal HER2 expression level) and 600,000 (high HER2 expression level).

5 Simulation Results and Model Predictions

In this section, we solve (8) numerically in Matlab using a standard stiff ODE numerical package (ode23s). In Sect. 5.1, we compare our numerical results against the experiments of Timms et al. (2002) and demonstrate that our model correctly captures the kinetics of EGFR-EGF-HER2 and transition rates in the G1/S phase of the cell cycle. In order to reproduce the experimental results and to calibrate our model, we need to vary some of the system parameters as described in Sect. 5.2. We then use experimental data of Hendriks et al. (2003a, 2003b) to make several new predictions concerning the growth advantage associated with increased level of HER2-receptors, as described in Sect. 5.3.

5.1 Comparing with Experimental Data

The first runs of the simulation return the percentages of cells in each compartment, i.e., %G1, %S, and %G2M, and the doubling time T_d for both HB4a and C3.6 cell

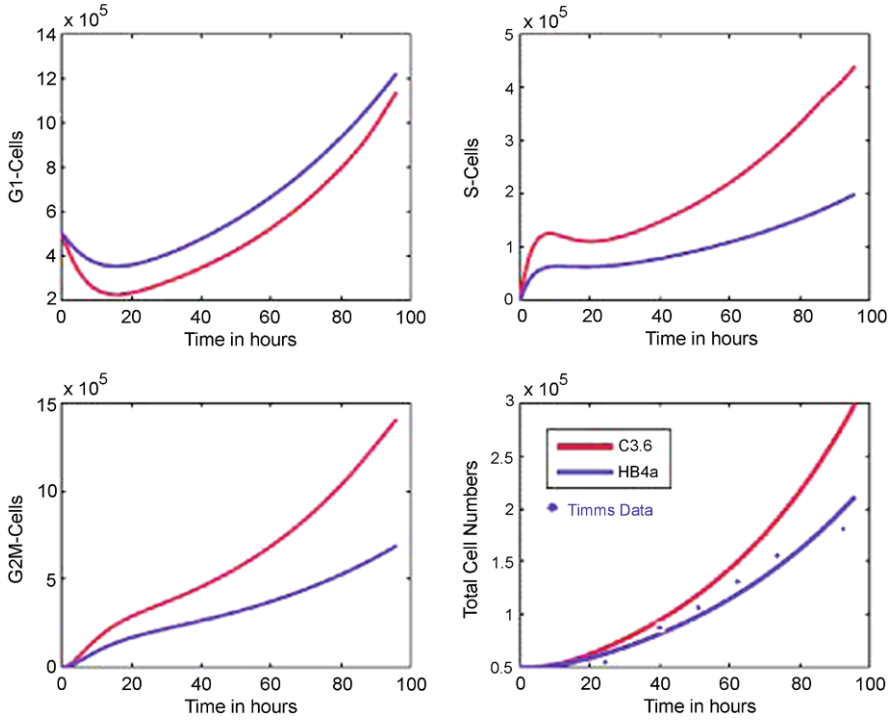

Fig. 2 Cell cycle dynamics. Parameter values used are: G1/S-transition ($\alpha_1^1 = \alpha_1^2 = 0.108$ hour^{-1}, $\beta_1^1 = \beta_1^2 = 4300$, $A_1 = 0.2$ ($B_1 = 0.8$)), and S/G2M transition ($\alpha_2^1 = \alpha_2^2 = 0.510$ hour^{-1}, $\beta_2^1 = \beta_2^2 = 4300$, $A_2 = 0.6$ ($B_2 = 0.4$)). Fixed values are: HB4a (HER2 = 10,000; EGFR = 10,000), C3.2 (HER2 = 100,000; EGFR = 100,000)

lines. These values are then used as inputs (in another computer program) to compute the various transition rates between cell cycle phases using Steels' equations (1).

Figure 2 shows the population dynamics of cells in G1-phase, S-phase, and G2M-phase and the total cell numbers. Figure 3 depicts a qualitative comparison between the flow cytometry data in Timms et al. (2002) and the simulation results for the parental cells HB4a and its clone cells C3.6. The following sets of values, describing transition dynamics of G1/S: ($\alpha_1^1 = 0.108$ hour^{-1}, $\beta_1^1 = 4300$, $A_1 = 0.2$) and of S/G2M: ($\alpha_2^1 = 0.510$ hour^{-1}, $\beta_2^1 = 4300$, $A_2 = 0.6$) are used to fit the experimental data. These sets of values reproduce results comparable to the exponential growth as in Timms' experiments. We note that the transient growth of the total cell population exhibits an exponential growth, which is consistent with the experimental data because some parameter values drive the cell population growth out of exponential growth regimen. For this particular simulation, the experimental data and the simulation results (summarized in Table 4) are in good agreement for C3.6 cells, as depicted in the cell cycle population histogram. However, we were not able to reproduce the results for the parental cells HB4a. The %G2M is close to the experimental values, but the %G1 is strongly underestimated, while the %S percentage is too high for the parental cells HB4a.

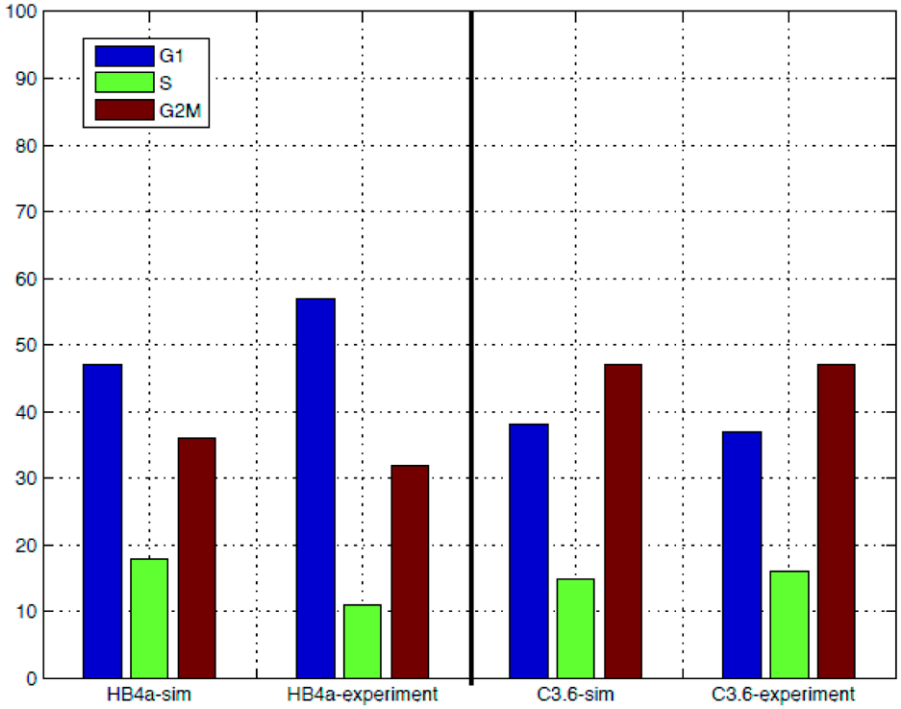

Fig. 3 Qualitative comparison of flow cytometry data and simulation results (same data as above)

Table 4 Cell-cycle percentages and transition rates: comparison between experimental data for the exponential growth (Timms et al. 2002) and simulation results

	HB4a				C3.6			
	T_d	%G1	%S	%G2M	T_d	%G1	%S	%G2M
Experiment	48	57	11	32	42	37	16	47
Simulation	48.48	47	18	36	42.67	38	15	47
Transition rates		λ_1	λ_2	λ_3		λ_1	λ_2	λ_3
Experiment		0.0430	0.1804	0.0520		0.0807	0.1597	0.0428
Simulation		0.0547	0.1150	0.0465		0.0771	0.1672	0.0422

We then varied other model parameters such as the maximum transition rates α_i^1 and the balancing factor A_i. The half-maximum constants β_i^1 are kept fixed at 4,600. With the following set of parameters: G1-phase to S-phase transition ($\alpha_1^1 = 0.108$ hour^{-1}, $\beta_1^1 = 4300$, $A_1 = 0.5$) and S-phase to G2M phase transition ($\alpha_2^1 = 0.570$ hour^{-1}, $\beta_2^1 = 4300$, $A_2 = 0.5$), the simulation results are consistent with the experimental data for HB4a cells (results listed in Table 5). In this simulation, we were not able to reproduce the results for C3.6 cells at the same time. We see that the

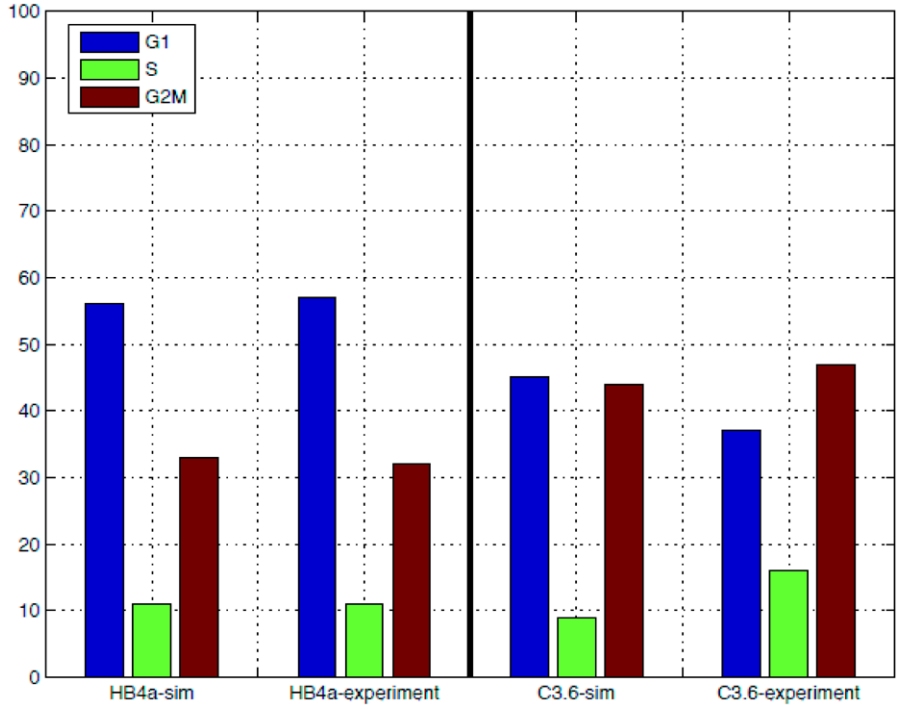

Fig. 4 Cell cycle population profile. Parameter values used are: λ_1 ($\alpha_1^1 = \alpha_1^2 = 0.108$ hour^{-1}, $\beta_1^1 = \beta_1^2 = 4300$, $A_1 = 0.5$ ($B_1 = 0.5$)), λ_2 ($\alpha_2^1 = \alpha_2^2 = 0.570$ hour^{-1}, $\beta_2^1 = \beta_2^2 = 4300$, $A_2 = 0.5$ ($B_2 = 0.5$)). Fixed values are: HB4a (HER2 = 10,000; EGFR = 10,000), C3.2 (HER2 = 100,000; EGFR = 100,000)

Table 5 Cell-cycle percentages and phase durations: comparison between experimental data for the exponential growth (Timms et al. 2002) and simulation results

	HB4a				C3.6			
	T_d	%G1	%S	%G2M	T_d	%G1	%S	%G2M
Experiment	48	57	11	32	42	37	16	47
Simulation	50	56	11	33	43	47	9	44
Transition rates		λ_1	λ_2	λ_3		λ_1	λ_2	λ_3
Experiment		0.0430	0.1804	0.0520		0.0807	0.1597	0.0428
Simulation		0.0431	0.1780	0.04960		0.0606	0.2680	0.0445

%G1 is over-estimated, the %S is under-estimated, while the %G2 is too poor. The cell cycle population profile for this simulation is depicted in Fig. 4.

Repeating the simulation with different biologically meaningful sets of parameters, was not successful in estimating a set of parameters that would fit the experimental data for both HB4a and C3.6 cells at the same time. We believe that this difference is likely due to the fact that our model assumes that the number of HER2 and EGFR

receptors to be identical in both G1 and S compartments. We have shown previously in Eladdadi and Isaacson (2008) that the cell proliferation model was sensitive to changes in the EGFR receptor numbers. Based on that information, we decided to vary the EGFR receptors numbers in the model simulation as shown below.

5.2 Parameter Variations

We now investigate the effect of varying EGFR expression level on the behavior of the system.

5.2.1 Effects of Varying EGFR in the Parental Cells HB4a

In this simulation, we use the same set of parameter values as discussed in the previous section (see Fig. 2). We proceeded by varying the EGFR receptors in G1 and S compartments separately. After repeated simulations, a value of 12,000 EGFR receptors in G1-phase, and a value of 4,000 EGFR receptors in S-phase yield similar results as in the experiments. The simulation results are summarized in Table 6. The cell cycle profile in Fig. 5 shows a very good approximation to the experimental data. This simulation resulted in a cell proliferation rate $\mu \simeq 0.01760$ hour^{-1} for HB4a cells and $\mu \simeq 0.01921$ hour^{-1} for C3.6 cells. That is $\approx$9% increase for the HER2 over-expressing cells C3.6 in comparison to its parental HB4a cells. Herein, we show that with these key parameter values reported in Table 6 the cell cycle model fits the experimental data and also predicts a growth advantage for the HER2-over-expressing cells.

5.2.2 Effects of Varying EGFR in the Clone Cells C3.6

Similarly, we vary the number of EGFR receptors in G1- and S-phases in C3.6 cells. We used the same set of parameter values described in the previous section (see Fig. 4). A range of 40,000 to 60,000 EGFR-receptors in S-phase gives a good fit for the experimental results with a doubling time $T_d \simeq 42.6$ hour. The number of the EGFR receptors in G1-phase was unchanged (100,000 receptors). The simulation results are summarized in Table 7, and the cell cycle profile is shown in Fig. 6.

This simulation resulted in a cell proliferation rates $\mu \approx 0.01663$ hour^{-1} for HB4a cells and $\mu \approx 0.01937$ hour^{-1} for C3.6 cells. That is $\approx$17% increase for the HER2 over-expressing cells C3.6 in comparison to its parental HB4a cells, confirming the growth advantage prediction for the HER2 over-expressing cells.

Many different combinations of the model input parameters gave very similar profiles (histograms) to those obtained experimentally (results not shown). Some combinations were eliminated because they resulted in biologically unrealistic doubling times. In our study, the simulated doubling time ranged from 48.48 hour to 51 hour for HB4a cells which is a good approximation with the experimental doubling time of 48 hour, and 42 hour to 43 hour for the clone, which is consistent with our previous model (Eladdadi and Isaacson 2008). In summary, with key parameter values, the simulation results show that HER2 over-expression results in a shorter G1-phase and early S-phase entry as shown in the cell population histograms. It also demonstrates

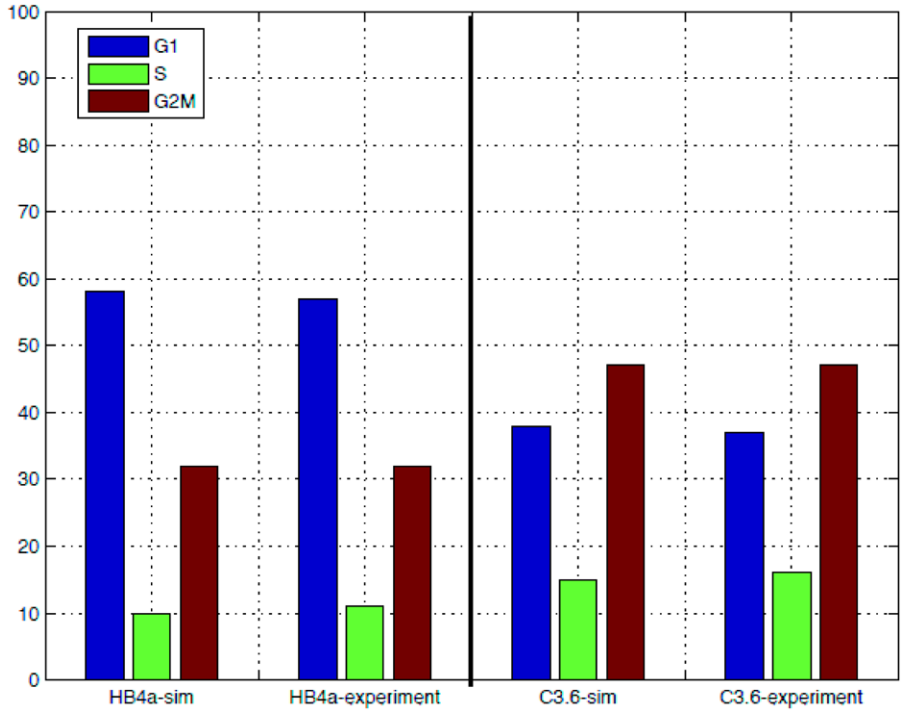

Fig. 5 Qualitative comparison of flow cytometry data and simulation results (same data as above)

Table 6 Varying the EGFR ratio in HB4a cells: Cell-cycle percentages and phase durations: comparison between experimental data for the exponential growth (Timms et al. 2002), and simulation results

	HB4a				C3.6			
	T_d	%G1	%S	%G2M	T_d	%G1	%S	%G2M
Experiment	48	57	11	32	42	37	16	47
Simulation	51	57	10	33	42.67	38	15	47
Transition rates		λ_1	λ_2	λ_3		λ_1	λ_2	λ_3
Experiment		0.0430	0.1804	0.0520		0.0807	0.1597	0.0428
Simulation		0.0405	0.1875	0.0477		0.0771	0.1672	0.0422

that "growth advantage" is associated with HER2 over-expression. This is consistent with the experimental data in Harris et al. (1999), Hynes (2005), Hynes et al. (2001), Timms et al. (2002).

5.3 Model Predictions

With these preliminary results at hand, we can proceed to other predictions that the model is able to make. Of particular interest are the growth advantage and the saturation effect associated with high level of the HER2.

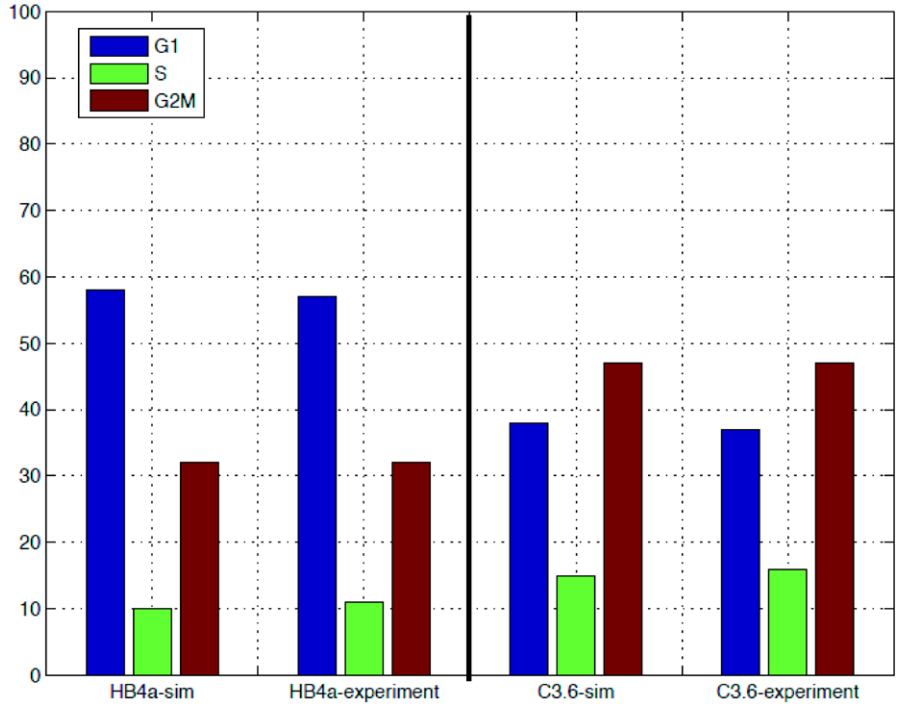

Fig. 6 Varying EGFR numbers in C3.6 cells: qualitative comparison of flow cytometry data and simulation results. Parameter values used are: λ_1 ($\alpha_1^1 = \alpha_1^2 = 0.108$ hour^{-1}, $\beta_1^1 = \beta_1^2 = 4300$, $A_1 = 0.5$), λ_2 ($\alpha_2^1 = \alpha_2^2 = 0.570$ hour^{-1}, $\beta_2^1 = \beta_2^2 = 4300$, $A_2 = 0.5$). C3.6 (HER2 = 100,000; EGFR($G1$) = 100,000; EGFR(S) = 60,000). Fixed values are: HB4a (HER2 = 10,000; EGFR = 10,000)

Table 7 Varying the number of EGFR receptors in C3.6 cells: Cell-cycle percentages and phase durations: comparison between experimental data for the exponential growth (Timms et al. 2002) and simulation results

	HB4a				C3.6			
	T_d	%G1	%S	%G2M	T_d	%G1	%S	%G2M
Experiment	48	57	11	32	42	37	16	47
Simulation	52	58	10	32	42.67	38	15	47
Transition rates		λ_1	λ_2	λ_3		λ_1	λ_2	λ_3
Experiment		0.0430	0.1804	0.0520		0.0807	0.1597	0.0428
Simulation		0.0400	0.1820	0.0480		0.0771	0.1672	0.0422

5.3.1 Growth Advantage

We use experimental data of Hendriks et al. (2003a), Hendriks et al. (2003b) to illustrate this positive correlation. We use our cell cycle model to simulate the cell proliferation of all the variants of the human mammary epithelial cell (HMEC) line

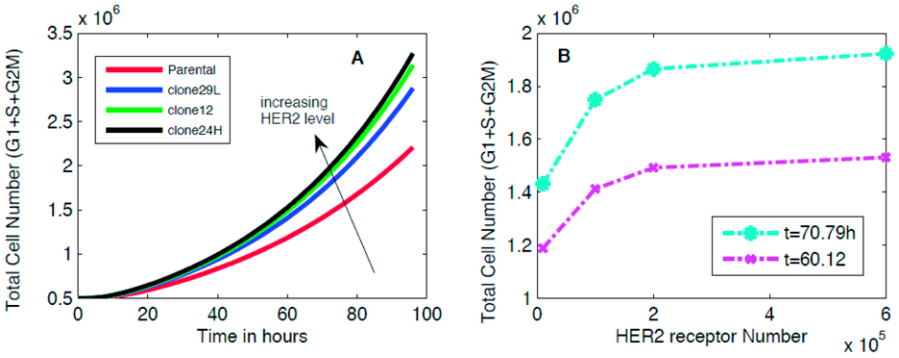

Fig. 7 (Color online) **A**: Growth Advantage Predictions for the HMEC 184A1 (1×10^4HER2—(*red*),) and its clones (1×10^5HER2—(*blue*), 3×10^5HER2—(*green*), 6×10^5HER2—(*black*)). **B**: Cell proliferation prediction. Parameter values used are: λ_1 ($\alpha_1^1 = \alpha_1^2 = 0.108$ hour^{-1}, $\beta_1^1 = \beta_1^2 = 4300$, $A_1 = 0.5$ ($B_1 = 0.5$)), λ_2 ($\alpha_2^1 = \alpha_2^2 = 0.570$ hour^{-1}, $\beta_2^1 = \beta_2^2 = 4300$, $A_2 = 0.5$ ($B_2 = 0.5$))

184A1. Herein, we compare the cell proliferation rates of the parental line "184A1" which expresses 10,000 HER2 per cell, to its three HER2 over-expressing clones: ("29L") that expresses 100,000 HER2; ("12") expresses 300,000 HER2; and ("24H") which expresses 600,000 HER2 Hendriks et al. (2003a), Hendriks et al. (2003b). We perform a series of simulations using the same set of parameters as in Fig. 6. However, for our model to account for the behavior depicted in Fig. 7A, we had to vary the number of EGFR receptors in both G1-phase and S-phase. We used a (1:1) ratio for the EGFR:HER2 (i.e., parental 184A1 (HER2 = 10,000; EGFR = 10,000), clone 29L (HER2 = 200,000; EGFR = 200,000), clone 12 (HER2 = 300,000; EGFR = 300,000), and clone 24H (HER2 = 600,000; EGFR = 600,000). Figure 7A depicts simulated cell population growth of 184A1 cell line and its clones (29L, 12, and 24H) at an EGF concentration of 100 nM (as in the experiments). These simulation results show that the rate of cell proliferation increases as the number of HER2 increases. The cell population growth rates of the parental cell line 184A1 and its clones computed from the log graph of Fig. 7A are as follows. Parental: $\mu = 0.016633$ hour^{-1}; clone (29L): $\mu = 0.019454$ hour^{-1}; clone (12): $\mu = 0.020374$ hour^{-1}; and clone (24H): $\mu = 0.02080$ hour^{-1}. The increase in the proliferation rate of the clones compared to the parental cell line 184A1 is approximately equal to 17% for clone 29L, ~22% for clone 12, and ~25% for clone 24H. These proliferation rates are consistent with those of our cell proliferation model (Eladdadi and Isaacson 2008).

5.3.2 Saturation Effect

These simulation results also show a "saturation" effect, that is, increasing HER2 and EGFR receptors beyond ~200,000 does not affect the cell proliferation rate, as seen for the clone 12 and clone 24H (Fig. 7A). On the basis of this information, we plotted the data from two time points as depicted in Fig. 7B. The simulation results exhibit a dose response dependence of cell proliferation rates on cell surface HER2 number. These results are consistent with our cell proliferation model described in

Eladdadi and Isaacson (2008). Furthermore, the simulation results are in agreement with earlier experimental studies conducted by Difiore et al. (1987), Harris et al. (1999), Timms et al. (2002). These studies show that HER2 over-expression results in increased mitogen-dependent proliferation in luminal epithelial cells, and that it is capable of transformation of the HER2 over-expressing cell lines to an extent and in a manner that correlates with the high level of HER2.

6 Discussion

In this paper, we presented a mathematical model to investigate how high expression levels of HER2 affect the cell cycle progression of HER2 over-expressing breast cancer cells. We used a three-compartment cell cycle model with nonconstant transition rates. Unique to this model is the dependence of the transition rates on HER2 and EGFR expression levels and their associated signaling kinetics. The model enabled us to simulate the transition rates of the HER2 over-expressing cells as they progress through their cell cycle with various HER2 and EGFR expression levels at various EGF ligand concentrations. The model also allowed for the prediction of the cell population growth as a function of HER2 and EGFR expression level. The model was validated using experimental observations in Timms et al. (2002). These experimental studies showed that HER2 over-expression contributed to the deregulation of the G1/S transition resulting in a shortening of the G1-phase and early S-phase entry of the cell cycle, which in turn yielded uncontrolled cell proliferation. Our main objective was to provide a quantitative description of these experimental observations in Timms et al. (2002) and to identify the key parameters which affect the regulation of the cell cycle in HER2 over-expressing cells. The major results from this model are highlighted below:

1. *Shorter G1 and early S-phase entry*: By judicious choice of the parameters, the simulations exhibit excellent agreement with the experimental results of Timms et al. (2002). The simulation results indicate that indeed HER2 over-expression leads to a shorter G1-phase and early entry to S-phase which results in hyperproliferation as reported in recent experimental studies by Harris et al. (1999), Hynes et al. (2001), Le et al. (2005).
2. *Growth advantage*: A key feature of this cell-cycle model is the growth advantage associated with the increase in the HER2-expression level. The model successfully interprets the experimental data for EGF-dependent growth of HB4a cell lines and its HER2 over-expressing clone C3.6. The numerical simulations show that, with key parameter values and with a 1-to-1 ratio between EGFR and HER2, the growth advantage in HER2-positive cells is indeed associated with high expression levels of HER2. This is consistent with previously published experimental studies (Harris et al. 1999; Timms et al. 2002) which confirm that HER2 over-expression leads to increased cell proliferation.
3. *Cell proliferation saturation*: The model realistically predicts a plateau in dose-response approaching saturation of cell population growth as a function of the cell surface HER2 number. Simulation results of the model revealed that there is a threshold of HER2 expression level that depends on ligand concentration and

above which HER2 levels have little effect on the cell proliferation. This finding is consistent with the experimental results in Hendriks et al. (2005) which showed that HER2 over-expression has no effect on ERK signaling ability when it is above a threshold value. ERK signaling is associated with the growth mechanism of one cell, which in turns translates into the rate of proliferation of the cell population.

4. *HER2 over-expression is an insufficient parameter*: One important finding of this model is that HER2 over-expression is an insufficient parameter to predict the proliferation response of cancer cells to epidermal growth factors. Our computer simulations show that EGFR expression level in HER2 over-expressing cells plays a key role in mediating the proliferation response to receptor-ligand signaling. This suggests that such synergies between the EGFR and HER2 contribute to the maintenance of increased proliferation rates associated with tumor development. This phenomenon correlates with the fact that not all HER2 positive patients treated with Herceptin respond to treatment (Baselga 2001; Baselga et al. 2006). Additionally, this finding is consistent with recently published experimental data about the improved efficiency, if both receptors are simultaneously targeted in breast cancer patients (Spector et al. 2005). Repeated simulations showed a sensitivity of the cell cycle model to HER2/EGFR ratio, indicating once more the importance of EGFR receptors in regulating cell proliferation in HER2 over-expressing cells. HER2 over-expressing cells with a ratio equal to 1, exhibited enhanced cell proliferation rates compared to similar cells with a ratio less than 1. This suggests that HER2-positive cancer patients with either a low or high HER2 /EGFR ratio will most benefit from taking into account both HER2 and EGFR receptors since tumor therapy can be adjusted to the individual coexpression profile. Taken together, the models' simulation results and current experimental data show that the contribution of EGFR receptor (as well as other HER receptors even though they were not included in this modeling attempt) should be taken into account for future evaluations of HER2 as a target for HER2 cancer therapy.

The original motivation for this and our previous work (Eladdadi and Isaacson 2008) was to investigate the effects of HER2 over-expression on cell proliferation and the cell cycle in breast cancer. Cancer growth is characterized by a variable cell cycle times that are controlled by stochastic events prior to DNA replication and cell division. In this paper, we have used a three-compartment cell cycle model with an exponential cell-cycle time distribution which is a simplistic representation of the cell cycle. Neither of these simplifications captures realistic cell-cycle time distributions compared to the cell cycle age-structured models. Age-structured models for the cell cycle are the simplest way to account for varied behavior of individual cells. However, age-structured models are difficult to fit to experimental data. They have been extensively studied (see, for example, Arino et al. 1997; Basse and Ubezio 2007; Bischoff et al. 1973; Brikci et al. 2008 and references therein). As additional experimental intracellular measurements for cell cycle regulatory proteins (such as microarray data, for example) become available, we expect to modify the model to a deterministic age-structured model.

This work serves as a first step in providing a quantitative understanding of how high expression levels of key receptors, HER2 and EGFR, and their associated signaling kinetics affect both the cell proliferation and cell-cycle transition rates.

Acknowledgements We thank the anonymous reviewers for their comments and suggestions which helped to improve the paper.

References

Alberts, B., Bray, D., Lewis, J., Raff, M., Roberts, K., & Watson, J. D. (2002). Cell growth and disvision. In *Molecular biology and cell biology* (4th ed.). New York: Garland.

Araujo, R. P., & Mcelwain, D. L. S. (2004). A history of the study of solid tumour growth: the contribution of mathematical modelling. *Bull. Math. Biol.*, *66*, 1039–1091.

Arino, O., Sanchez, E., & Webb, G. F. (1997). Necessary and sufficient conditions for asynchronous exponential growth in age structured cell populations with quiescence. *J. Math. Anal. Appl.*, *215*(2), 15.

Baselga, J. (2001). Herceptin alone or in combination with chemotherapy in the treatment of HER2-positive metastatic breast cancer: pivotal trials. *Oncology Suppl.*, *61*(2), 14–21

Baselga, J., Perez, E. A., Pienkowski, T., & Bell, R. (2006). Adjuvant trastuzumab: a milestone in the treatment of HER-2-positive early breast cancer. *Oncologist., 11*.

Basse, B., Baguley, B., Marshall, E., Wake, G., & Wall, D. (2005). Modelling the flow cytometric data obtained from unperturbed human tumour cell lines: Parameter fitting and comparison. *Bull. Math. Biol.*, *67*(4), 815–830.

Basse, B., & Ubezio, P. (2007). A generalised age- and phase-structured model of human tumour cell populations both unperturbed and exposed to a range of cancer therapies. *Bull. Math. Biol.*, *69*(5), 1673–1690.

Bischoff, K. B., Himmelstein, K. J., Dedrick, R. L., & Zaharko, D. S. (1973). Pharmacokinetics and cell population growth models in cancer chemotherapy. *Chem. Eng. Med.*, *1*, 47–64.

Brennan, P. J., et al. (2000). HER2/neu: mechanisms of dimerization/oligomerization. *Oncogene*, *19*, 6093–6101.

Brikci, F. B., Clairambault, J., & Perthame, B. (2008). Analysis of a molecular structured population model with possible polynomial growth for the cell division cycle. *Math. Comput. Model.*, *47*(7–8), 699–713.

Cai, Z., Zhang, G., Zhou, Z., Bembas, K., Drebin, J. A., Greene, M. I., & Zhang, H. (2008). Differential binding patterns of monoclonal antibody 2C4 to the ErbB3-p185her2/neu and the EGFR-p185her2/neu complexes. *Oncogene*, *27*, 3870–3874.

Cojocaru, L., & Agur, Z. (1992). A theoretical analysis of interval drug dosing for cell-cycle-phase-specific drugs. *Math. Biosci.*, *109*(1), 85–97.

Difiore, P. P., Pierce, J. H., Kraus, M. H., Segatto, O., King, C. R., & Aaronson, S. A. (1987). ErbB-2 is a potent oncogene when overexpressed in NIH 3T3 cells. *Science*, *237*, 178–182.

Eladdadi, A., & Isaacson, D. (2008). A mathematical model for the effects of her2 over-expression on the cell proliferation in breast cancer. *Bull. Math. Biol.*, *70*(6), 1707–1729.

Gorelik, B., Ziv, I., Shohat, R., Wick, M., Webb, C., Hankins, D., Sidransky, D., & Agur, Z. (2008). Efficacy of once weekly docetaxel combined with bevacizumab for patients with intense angiogenesis: validation of a new theranostic method in mesenchymal chondrosarcoma xenografs. *Cancer Res.*, *68*(21), 9033–9040.

Graus-Porta, D., et al. (1997). ErbB-2, the preferred heterodimerization partner of all ErbB receptors, is a mediator of lateral signaling. *EMBO J.*, *16*, 1647–55.

Harris, R. A., Eichholtz, T. J., Hiles, I. D., Page, M. J., & O'Hare, M. J. (1999). New model of ErbB-2 overexpression in fhuman mammary luminal epithelial cells. *Int. J. Cancer*, *80*, 477–484.

Hendriks, B., Opresko, L. K., Wiley, H. S., & Lauffenburger, D. A. (2003a). Quantitative analysis of HER2-mediated effects on HER2 and EGFR endocytosis: distribution of homo- and hetero-dimers depends on relative HER2 levels. *J. Biol. Chem.*, *278*, 23343–23351.

Hendriks, B., Wiley, H. S., & Lauffenburger, D. A. (2003b). HER2-mediated effects on EGFR endosomal sorting: analysis of biophyical mechanisms. *Biophys. J.*, *85*, 2732–2745.

Hendriks, B. S., Orr, G., Wells, A., Wiley, H. S., & Lauffenburger, D. A. (2005). Parsing ERK activation reveals quantitatively equivalent contributions from EGFR and HER2 in human mammary epithelial cells. *J. Biol. Chem.*, *280*, 6157–6169.

Howard, A., & Pelc, S. R. (1951). Nuclear incorporation of 32P as demonstrated by autoradiographs. *Exp. Cell Res.*, *2*, 178–187.

Hynes, N. E. (2005). Lane HA ERBB receptors and cancer: the complexity of targeted inhibitors. *Nat. Rev. Cancer*, *5*, 341–354.

Hynes, N. E., Horsch, K., Olayioye, MA, & Badache, A. (2001). The ErbB receptor tyrosine family as signal integrators. *Endocr. Relat. Cancer*, *8*, 151–159.

Klapper, L. N., Glathe, S., Vaisman, N., Hynes, N. E., Andrews, G. C., Sela, M., & Yarden, Y. (1999). The ErbB-2/HER2 oncoprotein of human carcinomas may function solely as a shared coreceptor for multiple stroma-derived growth factors. *PNAS*, *96*(9), 4995–5000.

Lane, H. A., Motoyama, A. B., Beuvink, I., et al. (2001). Modulation of p27/Cdk2 complex formation through 4D5-mediated inhibition of HER2 signaling. *Ann. Oncol. Suppl.*, *12*(1), S21–S22.

Le, X. F., Claret, F.-X., Lammayot, A., Tian, L., Deshpande, D., LaPushin, R., Tari, A. M., & Bast, R. C. Jr. (2003). The role of cyclin-dependent kinase inhibitor p27Kip1 in anti-HER2 antibody-induced G1 cell cycle arrest and tumor growth inhibition. *J. Biol. Chem.*, *278*, 23441–23450.

Le, X. F., Pruefer, F., & Bast, R. (2005). HER2-targeting antibodies modulate the cyclin-dependent kinase inhibitor p27Kip1 via multiple signaling pathways. *Cell Cycle*, *4*(1), 87–95.

Neve, R. M., Sutterluty, H., Pullen, N., Lane, H. A., Daly, J. M., Krek, W., & Hynes, N. E. (2000). Effects of oncogenic ErbB2 on G1 cell cycle regulators in breast tumour cells. *Oncogene*, *19*(13), 1647–1656.

Riese, D. J., & Stern, D. F. (1998). Specificity within the EGF family/ErbB receptor family signaling network. *BioEssays*, *20*, 41–48.

Salomon, D. S., Brandt, R., Ciardiello, F., et al. (1995). Epidermal growth factor-related peptides and their receptors in human malignancies. *Crit. Rev. Oncol./Hematol.*, *19*, 183–232.

Shapiro, H. M. (2003). *Practical flow cytometry* (4th ed.). Hoboken: Wiley-Liss.

Slamon, D. J., Clark, G. M., Wong, S. G., et al. (1987). Human breast cancer: correlation of relapse and survival with amplification of the HER-2/neu oncogene. *Science*, *235*, 177–182.

Spector, N. L., Xia, W., Burris, H., Hurwitz, H., Dees, E. C., Dowlati, A., O'Neil, B., Overmoyer, B., Marcom, P. K., Blackwell, K. L., Smith, D. A., Koch, K. M., Stead, A., Mangum, S., Ellis, M. J., Liu, L., Man, A. K., Bremer, T. M., Harris, J., & Bacus, S. (2005). Study of the biologic effects of lapatinib, a reversible inhibitor of ErbB1 and ErbB2 tyrosine kinases, on tumor growth and survival pathways in patients with advanced malignancies. *J. Clin. Oncol.*, *23*, 2502–2512.

Steel, G. G. (1977). *Growth kinetics of tumors: cell population kinetics in relation to the growth and treatment of cancer*. Oxford: Clarendon.

Takahashi, M. (1968). Theoretical basis for cell cycle analysis II: further studies on labelled mitosis wave method. *J. Theor. Biol.*, *18*, 195–209.

Timms, J. F., White, S. L., O'Hare, M. J., & Waterfield, M. D. (2002). Effects of ErbB-2 overexpression on mitogenic signalling and cell cycle progression in human breast luminal epithelial cells. *Oncogen*, *21*(43), 6573–6586.

Worthylake, R., Opresko, L. K., & Wiley, H. S. (1999). ErbB-2 amplification inhibits down-regulation and induces constitutive activation of both ErbB-2 and epidermal growth factor receptors. *J. Biol. Chem.*, *274*(13), 8865–8874.

Yarden, Y., & Sliwkowski, M. X. (2001). Untangling the ErbB signalling network. *Nat. Rev. Mol. Cell Biol.*, *2*, 127–137.